

Neurophotonics

Neurophotonics.SPIEDigitalLibrary.org

Rat embryonic hippocampus and induced pluripotent stem cell derived cultured neurons recover from laser-induced subaxotomy

Aaron Selfridge
Nicholas Hyun
Chai-Chun Chiang
Sol M. Reyna
April M. Weissmiller
Linda Z. Shi
Daryl Preece
William C. Mobley
Michael W. Berns

Rat embryonic hippocampus and induced pluripotent stem cell derived cultured neurons recover from laser-induced subaxotomy

Aaron Selfridge,^{a,*†} Nicholas Hyun,^{a,†} Chai-Chun Chiang,^b Sol M. Reyna,^c April M. Weissmiller,^b Linda Z. Shi,^d Daryl Preece,^e William C. Mobley,^b and Michael W. Berns^{a,d,f}

^aUniversity of California, San Diego, Department of Bioengineering, 9500 Gilman Drive, La Jolla, California 92093, United States

^bUniversity of California, San Diego, Department of Neurosciences, 9500 Gilman Drive, La Jolla, California 92093, United States

^cUniversity of California, San Diego, Department of Biomedical Sciences, 9500 Gilman Drive, La Jolla, California 92093, United States

^dUniversity of California, San Diego, Institute of Engineering in Medicine, 9500 Gilman Drive, La Jolla, California 92093, United States

^eUniversity of California, San Diego, Department of NanoEngineering, 9500 Gilman Drive La Jolla, California 92093, United States

^fUniversity of California, Irvine, Beckman Laser Institute, 1002 Health Sciences Road, Irvine, California 92612, United States

Abstract. Axonal injury and stress have long been thought to play a pathogenic role in a variety of neurodegenerative diseases. However, a model for studying single-cell axonal injury in mammalian cells and the processes of repair has not been established. The purpose of this study was to examine the response of neuronal growth cones to laser-induced axonal damage in cultures of embryonic rat hippocampal neurons and induced pluripotent stem cell (iPSC) derived human neurons. A 532-nm pulsed Nd:YVO₄ picosecond laser was focused to a diffraction limited spot at a precise location on an axon using a laser energy/power that did not rupture the cell membrane (subaxotomy). Subsequent time series images were taken to follow axonal recovery and growth cone dynamics. After laser subaxotomy, axons thinned at the damage site and initiated a dynamic cytoskeletal remodeling process to restore axonal thickness. The growth cone was observed to play a role in the repair process in both hippocampal and iPSC-derived neurons. Immunofluorescence staining confirmed structural tubulin damage and revealed initial phases of actin-based cytoskeletal remodeling at the damage site. The results of this study indicate that there is a repeatable and cross-species repair response of axons and growth cones after laser-induced damage. © 2015 Society of Photo-Optical Instrumentation Engineers (SPIE) [DOI: 10.1117/1.NPh.2.1.015006]

Keywords: growth cone; neurons; induced pluripotent stem cell; hippocampus; subaxotomy; regeneration.

Paper 14066R received Sep. 28, 2014; accepted for publication Jan. 12, 2015; published online Feb. 13, 2015.

1 Introduction

Neuronal growth cones are specialized motile structures that react to environmental cues to guide nerve growth during various stages of development. The repair and reassembly of the growth cones after injury is crucial to the process of nerve regeneration and is an important step in driving axonal reconnection with its target.^{1,2} Furthermore, the capacity to regenerate and properly reestablish connections has been shown to decrease with age.³ The regeneration of a new, functional axonal growth cone involves many intracellular processes, including proteolytic events, cytoskeletal rearrangement, and regulated transport of repair materials.⁴ Although progress has been made in identifying causes for abnormal regeneration, additional novel ways to study nerve repair and regeneration following injury can have a significant impact on our understanding of the process.

The focus of this study was to examine changes in growth cone morphology and movement in response to irradiation. Any mention of neuron activity, unless otherwise stated, is in reference to morphological changes rather than changes in electrical activity. To investigate the role of growth cones in nerve repair and regeneration, a laser microscope system was developed to locally damage axons while simultaneously observing the repair process in real time using phase and fluorescent microscopy. By

focusing a short-pulsed picosecond laser beam to a diffraction limited spot, individual axons in cell cultures can be manipulated without damaging adjacent cells. Previous studies have shown this approach to be feasible using cultured goldfish retinal ganglion cells.^{5,6} In these studies, goldfish nerve axons were partially damaged using a 532-nm nanosecond laser using a micropulse energy of 100 nJ without rupturing the cell membrane. Immediately after laser irradiation, nerve axons thinned at the lesion site and axonal repair was initiated.

Complete axotomy (as opposed to the subaxotomy described in this paper) of neurons *in vitro* has been performed with various laser systems and has been used to study the recovery of neurons *in vitro* and *in vivo*.^{7–9} Regeneration after complete axotomy involves a range of steps, which involve membrane resealing, cytoskeletal remodeling, and growth cone reformation.⁴ Repair following subaxotomy, however, likely utilizes previous growth cone components rather than the formation of a growth cone from new material and, thus, may be a significantly different damage repair process.⁵ Since recovery from laser subaxotomy does not involve several of the steps in the recovery from complete transection, such as membrane resealing, this method could be a valuable tool for the study of neural degeneration, repair, and regeneration.⁴ It is important, however, to demonstrate that these or similar processes occur in mammalian neurons. That is a key point of this study.

*Address all correspondence to: Aaron Selfridge, E-mail: arselfri@ucsd.edu; mwberns@uci.edu

†Authors contributed equally to this work.

Here, we employ laser subaxotomy in rat hippocampus and human induced pluripotent stem cell (iPSC) derived neurons. iPSC-derived neurons, in particular, are being used to model various neurodegenerative diseases with the hope that they may eventually be used in clinical management and treatment of neurological disorders. However, in-depth characterization of cellular function and repair processes in iPSCs and iPSC-derived neurons has not been done. Such characterization will help to provide a basis for the use of iPSC-derived neurons as a model for human neural systems.

In the study reported here, both hippocampal- and iPSC-derived neurons exhibit similar growth cone dynamics postlaser subaxotomy when analyzed by real-time quantitative imaging. The imaging methods, combined with immunofluorescence analysis, indicate that, in both human and rat models, growth cones play an active role in the repair of axonal injury and that this repair process requires cytoskeletal changes at both the site of injury and throughout the axon.

The results reported here, using two different mammalian neuronal systems, may help shed light on the damage-repair mechanisms of multiple neurological diseases and disorders, such as Alzheimer's disease and traumatic brain and spinal cord injury.

2 Materials and Methods

2.1 Primary Nerve Cell Preparation

Imaging dishes (MatTek) of 35 mm were coated with 0.2 mg/mL Poly-L-Lysine (PLL) solution and incubated for 3 h. PLL solution was aspirated and washed three times using culture grade water at 10-min intervals. Dishes were dried in a sterile hood before plating cells. Primary hippocampal neurons were dissected from embryonic 17- to 18-day rats and plated onto coated 35-mm imaging cell culture dishes as previously described.¹⁰ Briefly, hippocampi were dissected into Hanks balanced salt solution containing 10 mM HEPES and 1% penicillin/streptomycin. Following trypsin treatment and trituration, dissociated hippocampal neurons were plated at low density into imaging dishes with plating media (2% b27, 1% Glutamax, 5% fetal bovine serum in Neurobasal). The following day, the plating media was replaced with maintenance media (2% b27 1% Glutamax in Neurobasal). Neurons were fed fresh maintenance media every two to three days until the day of the experiment. Subaxotomy experiments on hippocampal neurons were performed three to six days postdissection.

2.2 iPSC-Derived Nerve Cell Preparation

Control iPSCs and neural progenitor cells (NPCs) derived from Craig Venter have been previously described.¹¹ Briefly, fibroblast biopsies were induced to a pluripotent state using the traditional Yamanka factors and expanded as iPSCs.¹² NPCs were made following published protocols by culturing iPSCs on a feeder layer of mouse stromal cells (PA6) for two weeks under conditions of dual SMAD inhibition.^{13,14} For neuronal differentiation, NPCs were seeded onto 10-cm plates coated with poly-ornithine and laminin (Sigma) and expanded as previously described in NPC media [Dulbecco's modified eagle medium:F12 + Glutamax, and 20 ng/ml Fibroblast growth factor (FGF) (Millipore)].^{11,14,15} After NPCs reached confluence, the FGF was removed from the NPC media to promote neuronal differentiation. At three weeks, cells were dissociated using Accutase and Accumax (Innovative Cell Technologies) and

resuspended in NPC media supplemented with 0.5 mM dibutyryl cyclic AMP (Sigma), 20 ng/ig brain-derived neurotrophic factor, and 20 ng/sg glial cell line-derived neurotrophic factor (Peprotech). In order to isolate true axons from the bulk culture, differentiated NPCs were seeded at a density of 2 million onto a microfluidic culture system coated with 100 $\mu\text{g}/\text{ml}$ poly-L-ornithine and 5 $\mu\text{g}/\text{ml}$ laminin (Sigma). Microfluidic culture systems have been shown to efficiently separate axons from soma and dendrites.^{16,17} A modified previously designed microfluidic system was used.¹⁸ Briefly, a central soma compartment (3 mm \times 100 μm \times 39 mm) is flanked by two open axon compartments (3 mm \times 23 mm \times 10 mm). The three compartments are connected by intermediate capillary channels (10 μm \times 3 μm \times 450 μm) that are thin enough to exclude soma and dendrites. After six to eight days, differentiated NPCs extend their axons through the capillary channels where laser subaxotomy is performed.

2.3 Tubulin Transduction and Immunofluorescence Staining

To visualize real-time cytoskeletal repair following laser subaxotomy, hippocampal neurons were transduced with tubulin tagged with red fluorescent protein (RFP). Cultures approximately three- to four-days old were incubated overnight with 10 μL of CellLight tubulin RFP (C10614, Life Technologies) and subsequently prepared for imaging. In order to examine tubulin and actin, some neurons were fixed with 4% paraformaldehyde for 1 h at room temperature immediately after subaxotomy. After PBS wash, fixed cells were incubated in a blocking buffer for 30 min and incubated overnight with the primary tubulin antibody (T9026, Sigma-Aldrich). The primary antibody was washed with PBS three times before incubating cells in the secondary antibody (A-11005, Life Technologies) against the mouse tubulin for 30 min. Neurons were then incubated for 20 min in Phalloiden (A12379, Life Technologies) diluted to 40:760 μL in PBS to stain for f-actin.

2.4 Laser Optical System

The optical system used in these studies has been described previously.^{19,20} Briefly, an Nd:YVO₄ 532-nm laser (Spectra-Physics, Vanguard) delivering 12-ps pulses at a 76-MHz repetition rate was used to create subaxotomies. The amount of laser power and energy entering the microscope was controlled using a polarizer mounted in a rotary mount (PR50PP, Newport Corp.). A mechanical shutter (Vincent Associates) with a 30 ms duty cycle gated the laser beam resulting in a 30-ms burst of pulses that entered the microscope and exposed the specimen at the laser focal point. A dual-axis fast scanning mirror (FSM-200-01, Newport Corp) was used to steer the laser beam at an image plane conjugate to the back focal plane of the microscope objective. At the specimen plane, the laser beam followed a linear path defined by the user (Fig. 1).

The amount of laser power/energy needed to create subaxotomy was determined by targeting an axon at a low laser power and gradually increasing the power until visible thinning of the axon was detected within a second after laser exposure. The pulse energy threshold to damage hippocampal neuronal axons was 0.351 nJ (peak irradiance 1.27×10^{11} W/cm²), while the pulse energy required to damage iPSC-derived neuronal axons was 0.268 nJ (peak irradiance of 0.97×10^{11} W/cm²). Only one to two 30-ms bursts of laser energy were exposed to the nerve

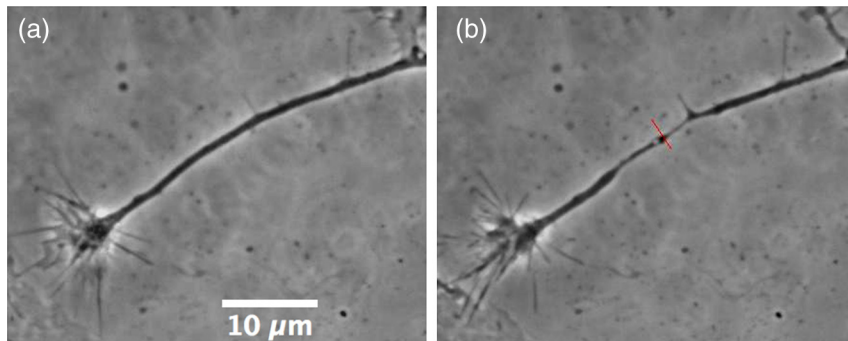


Fig. 1 Hippocampus axon with growth cone. An example subaxotomy experiment which shows the neuron at pre-laser (a) and post-laser (b). Axon thins [arrow in (b)] within 1 s after laser damage. Red line in (b) indicates the path of the laser beam.

axon since it is only a few microns in width. The total subaxotomy energy for one to two 30-ms bursts of laser exposure was 801 to 1602 μJ and 610 to 1220 μJ for hippocampal and iPSC-derived neurons, respectively.

2.5 Live Cell Imaging

The optical system utilized a Zeiss Axiovert 200M microscope with a 63X, phase NA 1.4 Plan-Apochromat oil immersion objective. Neurons were mounted on an X-Y stepper stage (Ludl Electronic Products). Phase and fluorescent images were acquired with a Hamamatsu Orca_AG deep-cooled 1344 \times 1024 pixel, 12-bit digital CCD camera.

To perform live imaging of neuronal cells for extended periods of time, the temperature (37°C), humidity, and CO₂ (5%) concentration of the environment was controlled using a microscope incubator (Okolab, NA, Italy). Once environmental conditions stabilized, neurons were placed in the microscope incubator and allowed to acclimate for 5 min. Neurons with established growth cones with active filopodia and lamellipodia were followed for 5 min using phase contrast imaging to characterize preirradiation morphology and behavior.

Axons were identified based on thickness, length, and morphology. Ideally, axons were more than 1 mm in length with a clear, active growth cone and no secondary extensions sprouting from the primary process.²¹ If no such processes were present, the longest process extending from the soma without branch points was targeted for laser irradiation. Based on these criteria, axons as opposed to dendrites, which are shorter thick processes with multiple branch points, were selected for subaxotomy. Phase contrast and fluorescent time series imaging were performed immediately and up to 60 min after axonal damage. Imaging was stopped when it was apparent that the recovery process was complete and the cell had stabilized. Based on morphological changes of the growth cone, the axonal damage site, and the cell body, it was determined that the cell had either returned to its pre-laser state or it did not recover from the laser damage. Possibly due to inherent cell variability (age, physiology, neuronal subtype, etc.), it was observed that different cells required different lengths of time to reestablish normal growth cone morphology and movement. Individual cells were followed for the period of time necessary to recover normal morphology, or until it was obvious that repair/recovery was no longer proceeding.

Images from pre- and post-laser exposure were compiled and analyzed using ImageJ. In order to quantitatively score growth cone recovery, a LabView program was written to analyze the

magnitude of the movement within and around the growth cone before and during the recovery process. The algorithm utilizes a wavelet transform to analyze the changes in an image series over time. Iterative application of temporal high- and low-pass filters allows for separation of the areas of the growth cone and axon, which are moving with high and low frequencies, and determine a concrete measurement of the magnitude of the oscillations at these frequencies.^{22,23} These magnitudes can then be plotted versus time as a relative measurement of growth cone activity before and after laser exposure. The measurements can also be used to characterize different classes of responses.

3 Results

3.1 Hippocampal Response

Phase contrast images of hippocampal neurons after laser subaxotomy showed a visible thinning of the axon followed by a repair process involving the growth cone and localized cytoskeletal remodeling (Figs. 2 and 3). Axons were scored qualitatively based on visible changes in morphology following laser exposure. A “++” response, which showed the highest level of recovery, was characterized by the return of the axon to its original thickness, with a recovery process involving either turning or retraction of the growth cone. A “+” response was a return to initial axon thickness without dynamic involvement of the growth cone. A “-” response was the degeneration of the axon and growth cone after laser damage. Completely transected neurons (axotomy) were noted and excluded from analysis. In 10 out of 23 axons imaged (Table 1, ++ response 47.82%), the growth cone retracted in the retrograde direction, extending filopodia toward the damage site (Figs. 2 and 3). The ++ response generally began 5 to 10 min after laser damage and had a duration of 17 ± 5 min.

In hippocampal neurons, 47.82% of the cells exhibited a ++ response, 43.48% a + response, and 8.7% of the neurons did not recover from the laser damage (Table 1). Of 23 damaged hippocampal neurons, 91.3% exhibited some level of repair and recovery, which involved growth cone and/or axonal remodeling.

Wavelet analysis of the growth cones using the LabView algorithm was used to identify and quantify the qualitative cell scoring of ++, +, and -. The activity trace for - cells, for example, shows a distinct drop-off as the growth cone activity decreases. Other responses, such as those seen in + or ++ cells, may decrease due to damage, but eventually return to near pre-cut levels, or they may not show significant decreases at all (Fig. 4).

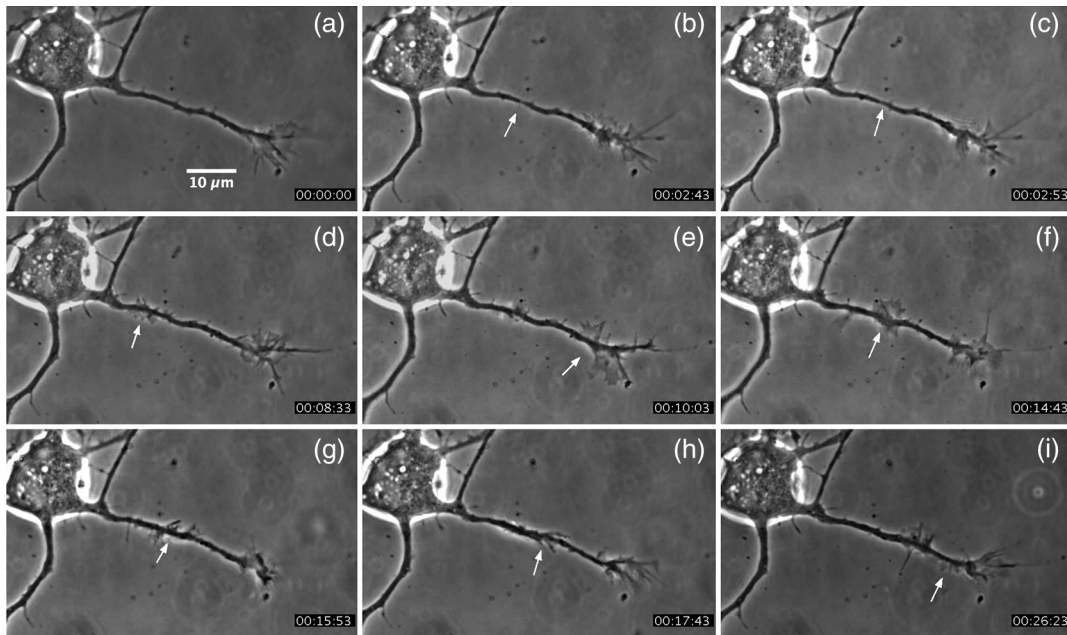


Fig. 2 Axonal growth cone dynamics of a representative rat-derived hippocampal neuron following sub-axotomy. Still frame images from a representative imaging session show several stages of injury, repair, and recovery. (a) Growth cone before laser subaxotomy. (b) The axon is damaged as indicated by the white arrow causing a thinning of the axon. (c) and (d) Axon is slightly thinner at ablation site and lamellipodia-like structures appear to form at the base of the cell body (arrow). (e) Growth cone retracts and lamellipodia-like components appear to be moving toward the damage site. (f) The growth cone is reduced in size. (g) and (h) Neuron axon thickens and returns to pre-laser morphology. (i) Lamellipodia progress forward and combine with the growth cone. See (Video 1 MOV, 6.46 MB) [URL: <http://dx.doi.org/10.1117/1.NPh.2.1.015006.1>], time series of laser induced damaged and recovery of hippocampus neuron.

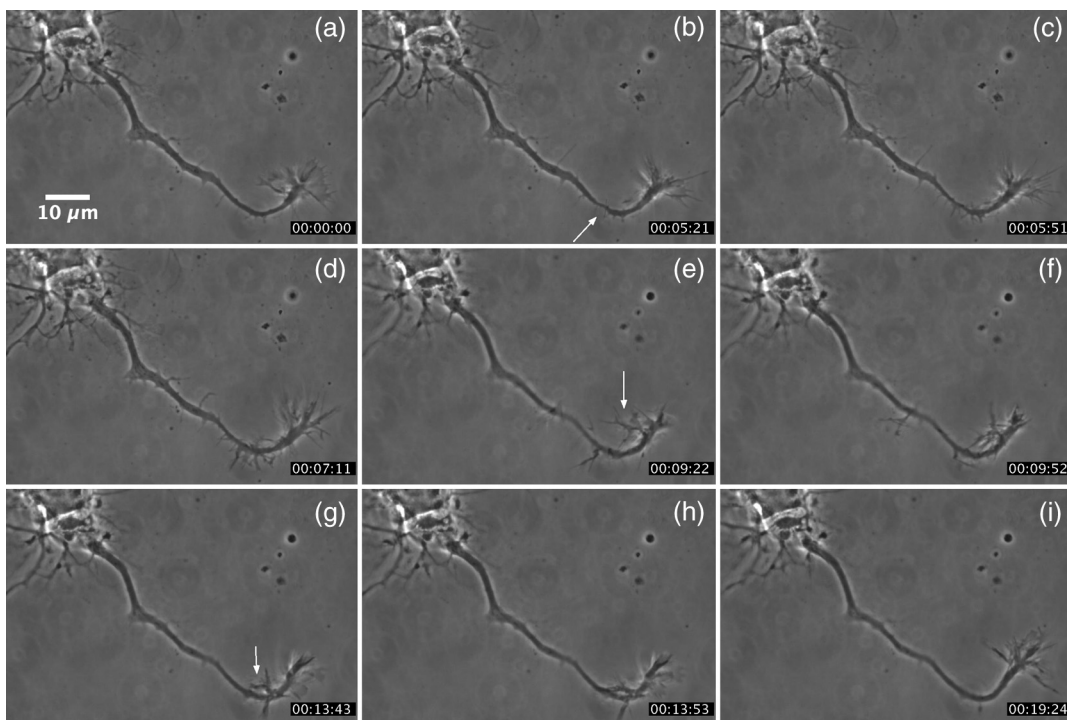


Fig. 3 Hippocampus growth cone turning in response to axonal damage. (a) Hippocampus nerve cell before laser ablation. (b) Nerve cell thinned at ablation site (arrow). (c) and (d) Filopodial-like structure forming at damage site. (e) to (h) Growth cone turning and extending filopodia toward the damage site. (i) Repaired axon. See (Video 2 MOV, 3.78 MB) [URL: <http://dx.doi.org/10.1117/1.NPh.2.1.015006.2>], time series of laser induced damaged and recovery of hippocampus neuron.

Table 1 Hippocampal neuron recovery. A “++” was assigned to neurons that displayed extensive axonal cytoskeletal remodeling as well as active involvement of the growth cone, “+” was assigned when repair occurred, without involvement of the growth cone, and “-” was assigned to neurons that did not recover from laser damage.

Response	Number	Percent
+	11	47.82
++	10	43.48
-	2	8.70
Total	23	100

Wavelet analysis was used to analyze the dynamics of the 23 hippocampal growth cones in this study. The low-frequency magnitude of the growth cone movement before subaxotomy was averaged, as was the magnitude for the last 100 s of the time series. The normalized recovery was calculated as follows:

$$\frac{\text{Average motion after cut} - \text{Average motion before cut}}{\text{Average motion before cut}}$$

Normalized recovery was plotted for each neuron (Fig. 5). Although the distribution for recovery is wide, the lowest

two points on the plot represent the two—scored cells. Based on these values, it is possible to estimate a threshold in movement, which separates—scored growth cones from + and ++ growth cones. This threshold can be approximated between -0.6 and -0.8, and is shown as -0.75 in Fig. 5.

Our live-imaging indicated large-scale changes in filopodia and lamellipodia dynamics along the axon, suggesting that cytoskeletal remodeling may be involved in repair after injury. Therefore, to examine the role of the cytoskeleton in the damage-repair process, two types of cytoskeletal elements, microtubules and actin, were examined. Microtubules are crucial for the axonal transportation system of a highly polarized neuron. Furthermore, actin is known to be a critical component of growth cone motility and dynamics, and is also essential in the formation of filopodia and lamellipodia.²⁴ Conventional immunofluorescence was used to determine if these two cytoskeletal components play a role in the changes observed during axonal repair. Hippocampus neurons were transiently transfected with RFP-tubulin. Fluorescently labeled RFP-tubulin was monitored before and after laser subaxotomy. Immediately after laser damage, the RFP-tubulin signal decreased in intensity at the damage site corresponding with the thinning observed in the phase contrast images. However, the RFP fluorescence recovered in intensity as axonal repair proceeded (Fig. 6). In addition, a visible retraction and accumulation of tubulin was observed at the damage site, consistent with the response seen in the phase contrast images. The results confirm that laser subaxotomy

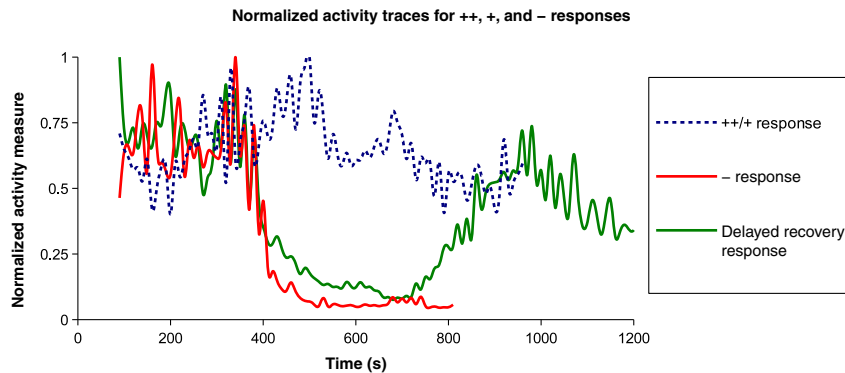


Fig. 4 High frequency (6 Hz) activity traces for different growth cones. “++” and “+” responses generally did not show a significant lasting change in activity and were similar. “-” responses were both characterized by a decrease in activity. An additional delayed response was observed in one case: activity decreased but did recover. Changes in growth cone morphology in the “-” time series indicated that no further increase in activity occurred after 800 s. In the above graph, laser subaxotomy occurred at 300 s. Values were normalized by division by the largest value in the time series.

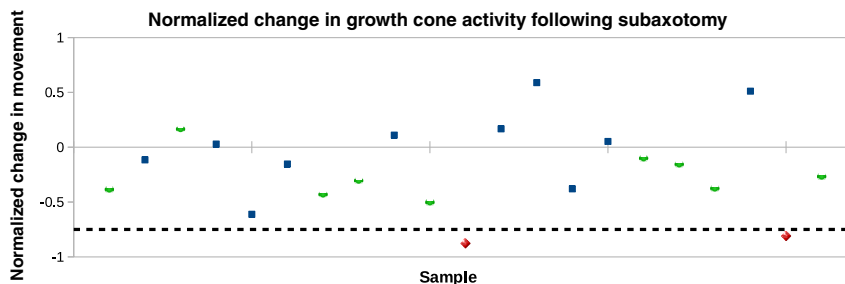


Fig. 5 The normalized change in movement for all growth cones, based on values before subaxotomy and values from the last 100 s of imaging. The two “-” cells fall below all other cells and appear to indicate a threshold for positive versus negative recovery, approximated by the line at -0.75. “++” cells are indicated as blue squares, “+” cells are indicated as green circles, and “-” cells are indicated as red diamonds.

structurally damages microtubules, and that microtubule function and/or polymerization may be an important step in the axonal repair process in the system studied here.

Cytoskeletal remodeling was also observed by fixing hippocampal neurons at different time points of recovery and staining for tubulin and actin. Thirteen cells were successfully damaged and stained. Immunofluorescent staining, while lacking the flexibility of transduction with fluorescent tagged actin and tubulin, provides stronger fluorescent signals and eliminates concerns of photobleaching and autofluorescence. The fixed immunofluorescent stains show a clear loss of tubulin at the laser ablation site, confirming the structural cytoskeletal damage caused by subaxotomy during live imaging analysis (Fig. 7, red channel).

In hippocampal neurons fixed 6 min after laser subaxotomy, fluorescent images showed morphological changes in the neuron's growth cone (Fig. 7, green channel). In addition, they showed visible accumulation of actin at the damage site consistent with the formation of lamellipodial-type structures during a ++ repair process. This suggests that formation of lamellipodia, and more specifically, changes in actin accumulation at the damage sites, may be an initial and important step in the axonal repair process.

One reported example of damage following subdendrotomy was an observed localized swelling at the damage site followed by either recovery or further degeneration. Although our experiments were on axons, rather than dendrites, parallels may exist

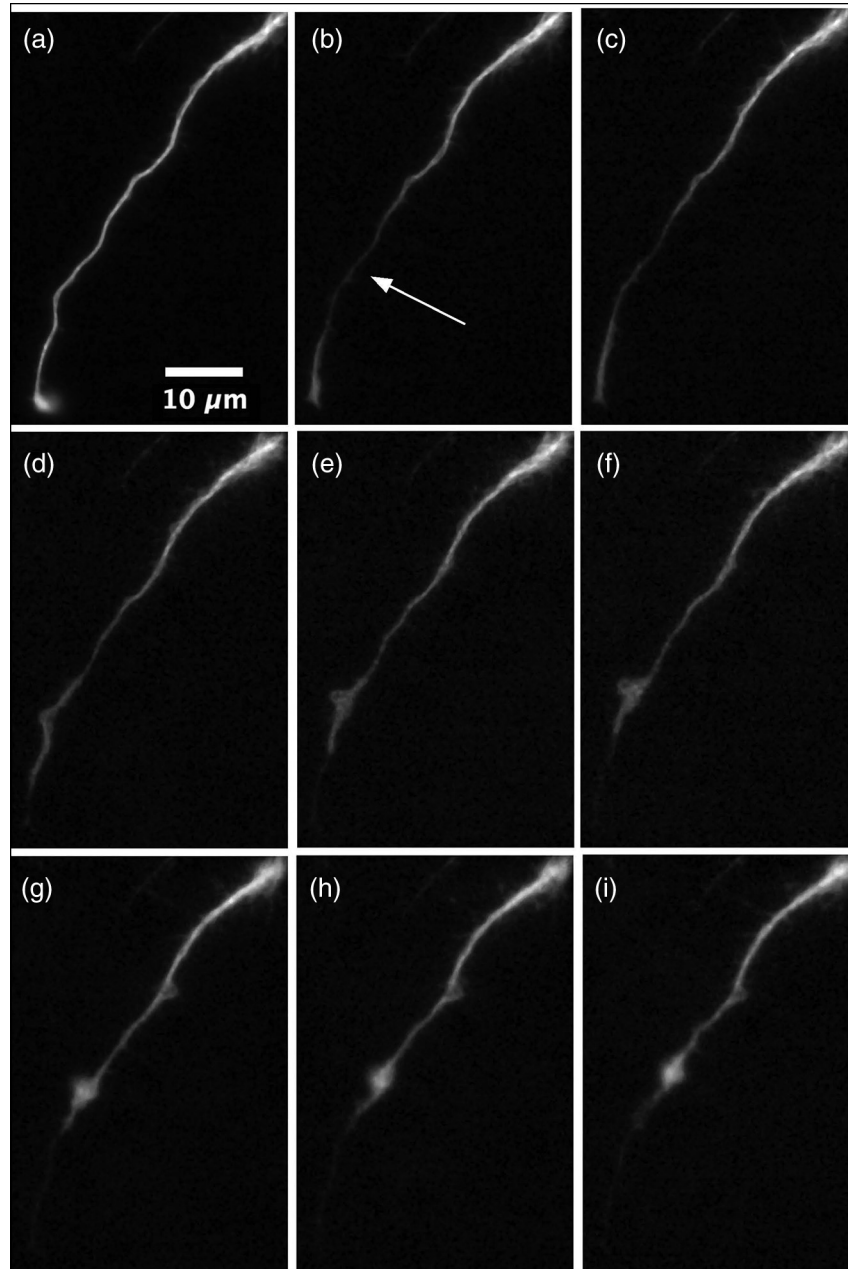


Fig. 6 Hippocampal neuron transduced with red fluorescent protein tubulin before and after laser radiation: (a) before laser radiation and (b) neuron immediately after laser radiation. Location of subaxotomy is indicated by the arrow. (c) and (d) Loss of tubulin near damage site. (e) and (f) Retraction of tubulin toward the damage site. (g), (h), and (i) Tubulin retraction continues and fluorescence at the damage site recovers.

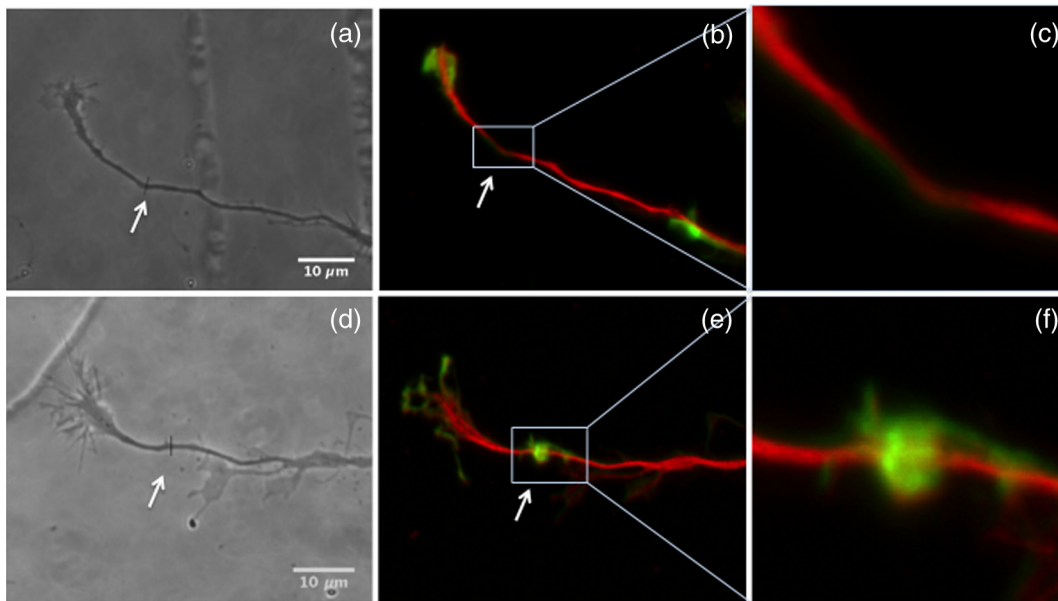


Fig. 7 Actin (green) and tubulin (red) staining of hippocampal neurons. (a) Phase contrast image of neuron prior to laser ablation. Location of cut indicated by the arrow. (b) Neuron fixed 5 min after cut. The arrow indicates the laser damage. (c) Zoomed image at the damage site. (d) Phase contrast image of neuron prior to laser ablation. Location of laser cut indicated by the arrow. (e) Neuron fixed 6 min after cut. The arrow indicates the laser damage. (f) Zoomed image at the damage site. See (Video 3 MOV, 1.98 MB) [URL: <http://dx.doi.org/10.1117/1.NPh.2.1.015006.3>], time series of laser induced damaged and recovery of iPSC-derived neuron.

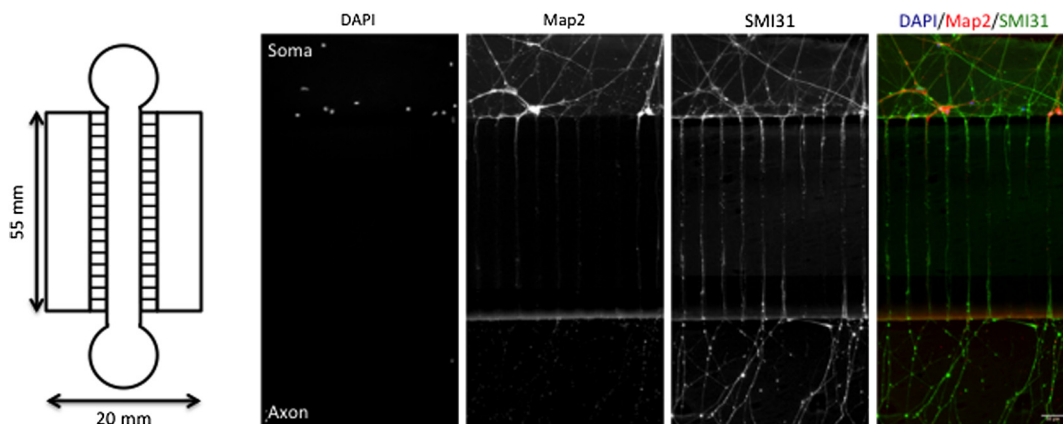


Fig. 8 Induced pluripotent stem cell (iPSC) derived neurons cultured in microfluidic compartmentalized chambers. Axonal marker SMI31 labels axonal compartment, while the somatodendritic marker Map2 labels only the cell body compartment. The nuclear marker DAPI clearly indicates which microfluidic well contains the cell body.

between the two.²¹ A proposed explanation for the swelling is that a change in membrane permeability following irradiation occurred, thus resulting in a change in osmotic equilibrium.⁷ Although irradiation likely changes plasma membrane properties in a number of ways, another explanation, based on the observed cytoskeletal dynamics, could be the occurrence of actin and/or tubulin accumulation as part of the remodeling process. The causes of axonal or dendritic swelling following irradiation may not be entirely attributed to either changes in osmotic balance or accumulation of cytoskeletal components.

3.2 Human iPSC-Derived Neuronal Response

iPSC-derived human neurons were studied in order to determine whether they exhibit axonal repair properties similar to the rat

hippocampus cells and the previous work on goldfish retinal ganglion neurons. iPSC-derived neurons were grown in compartmentalized chambers in which the axon could be separated from the cell body. As Fig. 8 shows, dendritic MAP2 staining remains in the cell body compartment, and axonal SM131 (phosphorylated neurofilament H) staining carries into the axonal compartment. Using this compartmentalized system, axons were easily identifiable from the rest of the cell. After laser subaxotomy a visible thinning was observed in the axon, similar to that observed in the rat hippocampal cells. The growth cones often retracted and appeared to shuttle membranous material in a retrograde direction toward the damage site, ultimately resulting in the formation of a varicosity at the site of laser damage (Fig. 9). Following this behavior, the iPSC-derived neurons

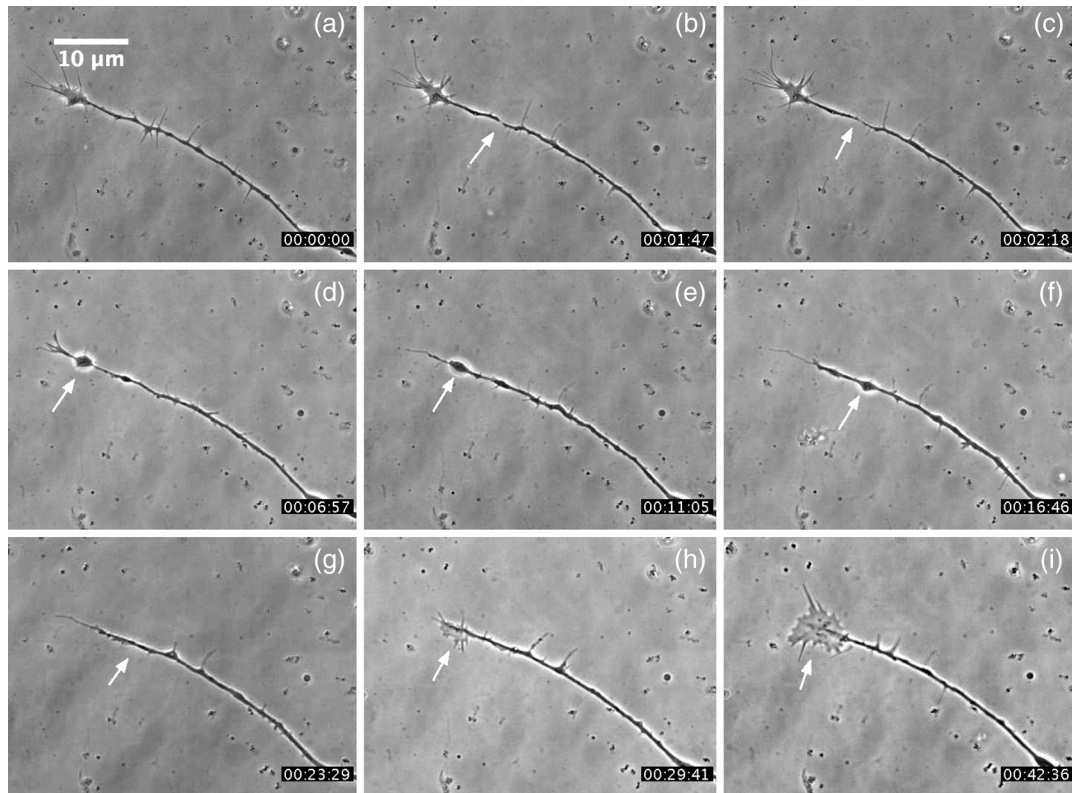


Fig. 9 iPSC-derived neuron repair and regeneration. (a) Neuron prior to laser ablation. (b) Arrow indicates site of laser damage. (b) and (c) Thinning at the damage. (d) to (f) Growth cone retracts toward damage site (arrows). (g) Axon shows no visible thinning (arrow). (h) and (i) Growth cone is re-established. See (Video 3 MOV, 1.98 MB) [URL: <http://dx.doi.org/10.1117/1.NPH.2.1.015006.3>], time series of laser induced damaged and recovery of iPSC-derived neuron.

reformed a growth cone with lamellipodial and filopodial extensions. The entire process of growth cone retraction, repair, and return to normal morphology took 40 ± 5 min. This process was two to three times as long as the repair process in rat brain hippocampal cells.

iPSC-derived neurons were also scored using a similar ranking system used previously for the rat hippocampal neurons. A ++ score was assigned to neurons that exhibited both axonal repair and growth cone reformation, + was assigned to neurons that exhibited axonal repair with partial or no reformation of growth cone, and – was assigned to neurons that did not recover from laser damage (Table 2). iPSC-derived neurons had a ++

Table 2 Induced pluripotent stem cell derived neuron recovery. A “+” score was assigned to neurons that exhibited both axonal repair and growth cone reformation, “+” was assigned to neurons that exhibited axonal repair with partial or no reformation of growth cone, and “–” was assigned to neurons that did not recover from laser damage.

Response	Number	Percent
+	7	25.00
++	6	21.40
–	15	53.60
Total	28	100

response of 18.5%, a + response of 25.9%, and a – response of 55.6%. Thus, of 27 damaged iPSC-derived neurons, 44.4% exhibited some level of repair and recovery to predamage morphology, about half of the rate recorded for rat-derived hippocampal neurons.

4 Discussion

The primary goal of this study was to determine if mammalian repair mechanisms following laser subaxotomy were similar to those observed in previously studied goldfish retina ganglion cells. Our results indicate that growth cone dynamics, and specifically cytoskeletal components, play significant roles in axonal recovery after laser subaxotomy in both hippocampal and iPSC-derived neurons. Of note, this is the first study demonstrating axonal injury recovery in an *in vitro* human, microfluidic compartment system, and paves the way for similar studies in iPSC-derived neurons modeling neurological diseases like Alzheimer’s disease, Rhett syndrome, Parkinson’s, etc. An additional novel feature of this study was the use of a wavelet transform algorithm to quantify the dynamic changes in growth cone remodeling in response to axonal damage. This quantification allows for a more in-depth analysis of the repair process. The quantification data presented here indicate that application of signal processing techniques produces repeatable measurements with direct bearing on ongoing physiological events. Furthermore, these measurements are fundamentally different from measurements based on growth cone area or number of filopodia as described by others.^{25,26}

The most striking difference between the iPSC and the rat hippocampus neurons was in regeneration rates. iPSC-derived neurons exhibited a – response 53.6% of time, whereas hippocampal neurons had – response of 8.7%, indicating that rat-derived hippocampal neurons were more likely to exhibit overt repair. The lower recovery rate of the iPSC-derived neurons could be due to a number of factors, including age of the culture. While growth cone dynamics in rat-derived neurons could easily be studied in the first week after dissection, the differentiation and plating process for human iPSCs is about four weeks (three weeks for differentiation followed by dissociation and replating in microfluidic devices). It has been shown that growth cones are more active and motile during early stages of development,^{4,27} therefore, the observed differences between the two cell systems may be due to developmental stage.

It is also possible that the distance of the damage site from the cell body plays a role in recovery. Subaxotomy was generally performed $\sim 10 \mu\text{m}$ distal to the growth cone. Damage further from the cell body may require longer time frames for movement of the necessary intracellular components via active transport or diffusion. The iPSC-derived neurons, having been cultured in microfluidic devices for long periods of time, generally had longer axons than the hippocampus neurons. Furthermore, human iPSC-derived neurons are not fully characterized and variations in neuronal subtype could be driving phenotype differences, though efforts to generate a more directed differentiation protocol are underway. The ability of iPSC-derived neurons to mimic normal neurons is an important prerequisite for their use as a model of degenerative disease and traumatic brain injury. Therefore, in the context of our study, it is relevant that human iPSC-derived neurons do exhibit mechanisms of axonal repair following laser subaxotomy.

In addition to affecting the regenerative potential of the cell, the location of the cut along the axon could affect the electrical activity of the neuron.²⁸ The axon initial segment has a high density of sodium channels and, likely, plays a role in action potential formation.⁸ As a result of laser subaxotomy, it is possible that the axon initial segment was damaged, resulting in more severe or otherwise different damage, compared to damage made at the end of the axon nearer the growth cone. Although changes in growth cone movement and morphology were the main focus of this study, normal electrical function will be an important parameter in order to establish functional neuron recovery. Future studies employing membrane potential sensitive dyes will be undertaken in an effort to determine if there is a positional relationship of the damage site with electrical activity.²⁹

The mechanisms of axonal damage by pulsed picosecond laser beams are not entirely understood, as they likely occur in the nonlinear optical regime. The relevant mechanisms may involve multiphoton generation of reactive oxygen and other free radicals, fragmentation of biomolecules by high electric fields, or photoablation similar to that observed in corneal sculpting procedures.³⁰ Laser irradiation may also generate a microplasma due to high photon density, but such events are unlikely since previous studies using similar irradiances did not rupture the axonal membrane, as would be expected with the generation of a plasma and the associated shock wave.^{5,31} Additionally, localized heating may play a role in the damage. However, since the laser exposure time is fast compared to the thermal rate of heat diffusion in water, it is unlikely that significant heat is generated outside the laser focal point. In previous

transmission electron microscope studies of the damaged site, no evidence of heating or plasma membrane damage was detected.⁵

The axonal thinning observed in hippocampus and iPSC-derived neurons with the 532-nm picosecond green laser beam was similar to the damage observed using a 532-nm nanosecond laser on goldfish retina neurons. Electron micrographs of the goldfish retina cells damaged with 532-nm laser showed that the damage did not rupture the cell membrane.⁵ In those studies, it appeared that the thinning was a result of loss of cytoskeletal structure in the axon even though there was evidence of some microtubules in the thinned area. The immunofluorescent studies described here support previous observations regarding the presence of tubulin at the damage site and extend these observations to include actin as a major component in the damage response. Further studies will determine the degree of tubulin and actin involvement in the neuronal repair process. Given the multitude of disorders and diseases exhibiting axonal dysfunction, it is important to determine the role of the cytoskeletal elements in the remodeling and repair of the damaged axon. In this paper, we demonstrate that laser subaxotomy provides a unique spatial and temporal modality for the production of axonal damage, which subsequently triggers a repair process in mammalian cells, including iPSC-derived neurons. In addition, we have combined immunofluorescent, genetic transduction, and quantitative methods to examine the damage-repair process in both iPSC-derived human neurons and rat hippocampus neurons.

5 Conclusion

This study revealed the dynamic axonal repair responses that are activated after laser-induced subaxotomy in mammalian cells, specifically rat hippocampal and human iPSC-derived neurons. This study also confirmed that actin and tubulin are involved in the damage response and recovery in neurons. Neural regeneration is a complex, multistep process. By eliminating several of the steps seen in recovery from complete axotomy, such as membrane resealing or formation of a new growth cone, laser subaxotomy is a more simplified model of neuronal repair following damage.⁴ Previous *in vivo* studies^{7–9} present compelling methods for the study of neural regeneration, but, due to the inherent complexity of *in vivo* systems, may not clearly distinguish the roles of individual pathways. The use of subaxotomy focuses on several key elements of neuronal response to damage.

The repair responses in the mammalian systems studied here were similar to those seen in previous studies on goldfish ganglion cells and suggest that the axon repair mechanisms are conserved over a range of species and distinct neuronal subtypes. Additional studies are needed to elucidate the biochemical pathways involved in growth cone sensing of damage and cytoskeletal remodeling, and to determine if the pathways are evolutionarily conserved. Experiments using fluorescent dyes or forster resonance energy transfer-based biosensors will be useful in the elucidation of the intracellular signaling pathways involved in sensing and repair of axonal damage.³² In addition, several inhibitors, such as cytochalasin D,³³ Nocodazole,³⁴ and ROCK,³⁵ will be used in future studies involving cytoskeletal remodeling following laser subaxotomy. In conclusion, laser subaxotomy at the single-cell level can contribute to an understanding of the repair mechanism necessary to restore damaged neuronal circuits at the tissue and organ levels.

Acknowledgments

This work was supported by AFOSR Grant # FA9550-08-1-0384 and funds from the Beckman Laser Institute Inc. Foundation awarded to M. W. B., as well as Lumind Grant # 20150097 awarded to Dr. William Mobley, Research Down Syndrome Foundation Grant # 20150489 awarded to Dr. William Mobley, Nanomedicine Grant # 5PN2EY016525 sub-awarded to Dr. William Mobley, and R01 with Roswell Park Grant # 5R01NS066072-05 awarded to Dr. William Mobley and Dr. Eugene Yu.

References

1. V. J. Tom et al., "Studies on the development and behavior of the dystrophic growth cone, the hallmark of regeneration failure, in an *in vitro* model of the glial scar and after spinal cord injury," *J. Neurosci.* **24**(29), 6531–6539 (2004).
2. A. Erturk et al., "Disorganized microtubules underlie the formation of retraction bulbs and the failure of axonal regeneration," *J. Neurosci.* **27**(34), 9169–9180 (2007).
3. Z. Wu et al., "Caenorhabditis elegans neuronal regeneration is influenced by life stage, ephrin signaling, and synaptic branching," *PNAS* **104**(38), 15132–15137 (2007).
4. F. Bradke, J. W. Fawcett, and E. S. Spira, "Assembly of a new growth cone after axotomy: the precursor to axon regeneration," *Nat. Rev. Neurosci.* **13**(3), 183–193 (2012).
5. T. Wu et al., "Neuronal growth cones respond to laser-induced axonal damage," *J. R. Soc. Interface* **9**(68), 535–547 (2012).
6. T. Wu et al., "A photon-driven micromotor can direct nerve fibre growth," *Nat. Photonics* **6**, 62–67 (2012).
7. A. Mascaró, L. Sacconi, and F. S. Pavone, "Multi-photon nanosurgery in live brain," *Front. Neuroenergetics* **2**(21) (2010).
8. M. Kole, "First node of Ranvier facilitates high-frequency burst encoding," *Neuron* **71**(4), 671–682 (2011).
9. A. Mascaró et al., "In vivo single branch axotomy induces GAP-43-dependent sprouting and synaptic remodeling in cerebellar cortex," *PANS* **110**(26), 10824–10829 (2013).
10. J. Wan et al., "Endophilin B1 as a novel regulator of nerve growth factor/TrkA trafficking and neurite outgrowth," *J. Neurosci.* **28**(36), 9002–9012 (2008).
11. G. Woodruff et al., "The Presenilin-1 $\Delta E9$ mutation results in reduced γ -Secretase activity, but not total loss of PS1 function, in isogenic human stem cells," *Cell Reports* **5**(4), 974–985 (2013).
12. K. Takahashi et al., "Induction of pluripotent stem cells from adult human fibroblast by defined factors," *Cell* **131**(5), 861–872 (2007).
13. S. M. Chambers et al., "Highly efficient neural conversion of human ES and iPS cells by dual inhibition of SMAD signaling," *Nat. Biotechnol.* **27**, 275–280 (2009).
14. S. H. Yuan et al., "Cell-surface marker signatures for the isolation of neural stem cells, glia and neurons derived from human pluripotent stem cells," *PLoS ONE* **6**(3), e17540 (2011).
15. M. A. Israel et al., "Probing sporadic and familial Alzheimer's disease using induced pluripotent stem cells," *Nature* **482**, 216–220 (2012).
16. A. M. Taylor et al., "A microfluidic culture platform for CNS axonal injury, regeneration and transport," *Nat. Methods* **2**(8), 599–605 (2005).
17. A. M. Taylor et al., "Microfluidic local perfusion chambers for the visualization and manipulation of synapses," *Neuron* **66**(1), 57–68 (2010).
18. E. M. Niederst, S. M. Reyna, and L. S. Goldstein, "Axonal amyloid precursor protein and its fragments undergo somatodendritic endocytosis and processing," *Mol. Biol. Cell* **14**(06), 1049 (2014).
19. E. L. Botvinick and M. W. Berns, "Internet-based robotic laser scissors and tweezers microscopy," *Microsc. Res. Tech.* **68**, 65–74 (2005).
20. L. Z. Shi, M. W. Berns, and E. Botvinick, "RoboLase: Internet-accessible robotic laser scissor and laser tweezers microscope system," in *Medical Robotics*, V. Bozovic, Ed., pp. 401–420, I-Tech Education and Publishing, Vienna, Austria (2008).
21. M. D. Ledesma and C. G. Doti, "Membrane and cytoskeleton dynamics during axonal elongation and stabilization," *Int. Rev. Cytol.* **227**, 183–219 (2003).
22. D. Davies, P. Palmer, and M. Mirmehdi, "Detection and tracking of very small low contrast objects," in *Proc. British Machine Vision Conf.*, M. Nixon and J. Carter, Eds., pp. 60.1–60.10, BMVA Press (1998).
23. R. Strickland, "Wavelet transform methods for object detection and recovery," *IEEE Trans. Image Process.* **6**(5), 724–735 (1997).
24. R. M. Gomez and P. C. Letourneau, "Actin dynamics in growth cone motility and navigation," *J. Neurochem.* **129**(2), 221–234 (2014).
25. C. Portera-Cailliau, D. T. Pan, and R. Yuste, "Activity-regulated dynamic behavior of early dendritic protrusions: evidence for different types of dendritic filopodia," *J. Neurosci.* **23**(18), 7129–7142 (2003).
26. S. Nilufar et al., "FiloDetect: automated detection of filopodia from fluorescence microscopy images," *BMC Syst. Biol.* **7**(66) (2013).
27. E. W. Dent and F. B. Gertler, "Cytoskeletal dynamics and transport in growth cone motility and axon guidance," *Neuron* **40**(2), 209–227 (2003).
28. K. J. Fernandes et al., "Influence of the axotomy to cell body distance in rat rubrospinal and spinal motor neurons: differential regulation of GAP-43, tubulins, and neurofilament-M," *J. Comp. Neurol.* **414**(4), 495–510 (1999).
29. R. S. Bedlack, M. Wei, and L. M. Lowe, "Localized membrane depolarizations and localized calcium influx during electric field-guided neurite growth," *Neuron* **9**(3), 393–403 (1992).
30. M. Niemz, *Laser-Tissue Interactions: Fundamentals and Applications*, Springer, Berlin-Heidelberg (2007).
31. A. Vogel et al., "Mechanisms of femtosecond laser nanosurgery of cells and tissues," *Appl. Phys. B* **81**(8), 1015–1047 (2005).
32. K. Okamoto et al., "Rapid and persistent modulation of actin dynamics regulates postsynaptic reorganization underlying bidirectional plasticity," *Nat. Neurosci.* **7**(10), 1104–1112 (2004).
33. S. M. Kim et al., "Control of growth cone motility and neurite outgrowth by SPIN90," *Exp. Cell Res.* **317**(16), 2276–2287 (2011).
34. P. Charoenkwan et al., "HCS-Neurons: identifying phenotypic changes in multi-neuron images upon drug treatments of high-content screening," *BMC Bioinformatics* **14**(Suppl 16), S12 (2013).
35. M. Takata et al., "Fasudil, a rho kinase inhibitor, limits motor neuron loss in experimental models of amyotrophic lateral sclerosis," *Br. J. Pharmacol.* **170**(2), 341–351 (2013).

Aaron Selfridge is an undergraduate student at UCSD studying bioengineering, whose work focuses on the mechanics of neural regeneration. His interests include developing and applying microfluidic and optical systems to neuroscience in order to address medically relevant issues.

Nicholas Hyun obtained his master's degree in bioengineering from the University of California, San Diego (UCSD). The focus of his work was the application of optical and laser systems in biological research, including sperm motility and neuron regeneration.

Chai-Chun Chiang obtained her MD degree from National Yang Ming University, School of Medicine in Taipei, Taiwan. After graduation, she worked as a postdoctoral research scholar in Dr. William Mobley's lab at UCSD, Department of Neurosciences. Currently, she is doing her neurology residency training at Mayo Clinic in Arizona. Her research interests include using bioengineering methods to study neuroscience and neurological diseases. Her ultimate goal is to become a physician scientist.

Sol M. Reyna is a molecular neuroscientist working on induced pluripotent stem cell derived neuronal models of Alzheimer's disease in Dr. Goldstein's laboratory at UCSD. She is interested in understanding the role of altered endocytosis, transcytosis, and axonal transport in familial Alzheimer's disease mutations in a human neuronal system.

April M. Weissmiller observed that advances in understanding the biology of neurotrophic factors and their signaling pathways have provided important insights into the normal growth, differentiation, and maintenance of neurons. Stimulated by neuropathological observations and genetic discoveries, studies in cell and animal models of neurodegenerative disorders have begun to clarify pathogenetic mechanisms of disease. Her research examines the intersection of these research themes and identifies several potential mechanisms for linking failed neurotrophic factor signaling to neurodegeneration.

Linda Z. Shi is a project scientist at the Institute of Engineering in Medicine and the lab manager at Biophotonics Lab at UCSD. Her research interests include the software design and hardware implementation for robotic laser microscope systems, DNA repair mechanics, and sperm motility.

Daryl Preece works as a project scientist in the cellular biophotonics group. He is an expert in holographic optical trapping and optical forces. His focus is on novel mechanisms on light–matter interaction. His current interests include the interaction of optical forces with live cells.

William C. Mobley is chair of the Department of Neurosciences at UCSD and director of the Down Syndrome Center for Research

and Treatment at UCSD. Before moving to UCSD in 2009, he was professor and chairman of the Department of Neurology and Neurological Sciences at Stanford, where he directed Stanford's Center for Research and Treatment of Down Syndrome.

Michael W. Berns is the Arnold and Mabel Beckman professor in the Departments of Biomedical Engineering, Surgery, and Developmental and Cell Biology at UC Irvine, where he is the founding director of the Beckman Laser Institute. He is an adjunct professor of bioengineering and member of the Institute for Engineering in Medicine at UCSD. He has pioneered the use of laser scissors and tweezers to manipulate cells and their organelles.